224
9/19/89 JS ③

SANDIA REPORT

SAND89–1197 • UC–510
Unlimited Release
Printed September 1989

Quasi-Static and Dynamic Mechanical Properties of a Granite and a Sandstone

DO NOT MICROFILM
COVER

William A. Olsson

Prepared by
Sandia National Laboratories
Albuquerque, New Mexico 87185 and Livermore, California 94550
for the United States Department of Energy
under Contract DE-AC04-76DP00789

Issued by Sandia National Laboratories, operated for the United States Department of Energy by Sandia Corporation.

Printed in the United States of America. This report has been reproduced directly from the best available copy.

Available to DOE and DOE contractors from
Office of Scientific and Technical Information
PO Box 62
Oak Ridge, TN 37831

Prices available from (615) 576-8401, FTS 626-8401

Available to the public from
National Technical Information Service
US Department of Commerce
5285 Port Royal Rd
Springfield, VA 22161

NTIS price codes
Printed copy: A02
Microfiche copy: A01

August 30, 1989

Distribution
Category UC-510

SAND--89-1197

DE89 016963

Quasi-Static and Dynamic Mechanical Properties of a Granite and a Sandstone*

William A. Olsson

Geomechanics Division
Sandia National Laboratories
Albuquerque, New Mexico 87185

ABSTRACT

The quasi-static failure criteria, elastic constants, and p-wave velocities have been determined for a granite and a sandstone in which blasting experiments are being carried out by the Advanced Technology Division (6258). In addition, the dynamic strength of the granite was measured using a Kolsky bar. Both rocks show a linear increase in strength with increasing confining pressure. The dynamic strength of the granite is as much as 330% greater than the quasi-static value. The strength of the granite was also dependent on the angle between the foliation and the loading direction. There was a 20% difference in the p-wave velocity between that measured parallel to and perpendicular to the bedding in the sandstone.

*This work performed at Sandia National Laboratories supported by the U.S. Department of Energy under contract number DE-AC04-76DP00789.

Contents

List of Figures

List of Tables

1 Introduction

Improvements in the technology of rock blasting are being made by the Advanced Technology Division (6258) through the integration of field experiments and computer simulation. Constitutive data required in the calculations and reported herein are being collected in the Geomechanics Division (6232). The specific data needs are the elastic moduli, pressure-dependent failure criteria, and dynamic strengths. Accordingly, tests have included uniaxial compression, triaxial compression, hydrostatic compression, and compression tests under impulsive loading. Attention was also given to developing a dynamic tensile test for use in the applicable strain-rate regime; the results will be reported separately.

2 Materials and Experimental Procedures

Two rocks in which blasting experiments were being carried out were tested: a granite from North Carolina, and a sandstone from Kentucky. The granite samples were taken from the muck pile from cratering experiments. The sandstone was taken from exploratory drill holes. An accurate petrographic description is not available for either rock.

The strength and elastic moduli were measured in electro-hydraulic, servo-controlled testing machines manufactured by *MTS Systems, Inc.* Axial deformations were measured with two linear variable differential transformers (LVDT's) attached directly to the samples. The lateral deformations were measured with an LVDT held in a fixture designed by Holcomb and McNamee [1984]. Axial force was measured with a load external to the confining pressure vessel. The axial displacement rates were held constant throughout the quasi-static testing and corresponded to strain rates of approximately 10^{-4} s^{-1}. Samples tested under confining pressure were jacketed in heat-shrinkable, polyolefin tubing. The dynamic strengths were measured in a Kolsky bar (Kolsky, 1949) at strain rates from 113 to 192 s^{-1}.

All samples were core drilled with water as coolant, and centerless ground. Samples were tested in the air-dry condition. Sandstone samples were 50.8 mm in diameter and 101.6 mm in length. The granite samples were 25.4 mm in diameter and 50.8 mm in length. Because the granite had a visible layering, cores were taken with their axes at 30 and 90 degrees to the layering. The sandstone bedding was defined by irregular, subhorizontal, dark-colored streaks. These layers may also define a mechanical anisotropy, but no measurements were made of strength in different directions for the sandstone.

The test data were collected on a *Digital Equipment Corporation LSI 11/23* computer using software described in Holcomb and Jones [1983]. Data thus collected were then transferred to a *VAX 8700* (*Digital Equipment Corporation*) for analysis using software written by D. J. Holcomb (6232) and plotting using *GRAPH II* [Selleck, 1984].

In the tables at the end of this report, the angle between the layering and the loading direction is denoted by θ; density by ρ; maximum and minimum compressive stresses by σ_1 and σ_3, respectively; Young's modulus by E; Poisson's ratio by ν; p-wave velocity parallel to layering by $v_{\|}$, and normal to layering by $v_{\perp}$.

3 Results

3.1 Sandstone

The densities, p-wave velocities, and depth interval for the sandstone are listed in Table 1. The difference between velocity measured perpendicular ($v_{\perp}$) and velocity measured parallel to layering ($v_{\|}$) is quite noticeable, about 19 %. This is attributed to the dark irregular layering oriented perpendicular to the core axis.

The stress-strain data for the sandstone are shown in Figure 1. The samples tested at all confining pressures were elastic only initially and showed a gradually decreasing tangent modulus to zero at the ultimate stress (strength). Beyond the ultimate stress, all but one sample exhibited rapid loss of strength resulting from faulting. Prior to faulting, each sample developed well-defined slip lines on the surface. The fact that one sample at 200 MPa confining pressure showed no stress drop and did not develop a fault, and that the other sample tested at that pressure showed only a small stress drop, indicates that 200 MPa is near to the phenomenological brittle-ductile transition pressure. This implies that at confining pressures above 200 MPa, the stress-strain curve would show little or no stress drop, and faulting would be replaced by a more homogeneous mode of deformation. Under these circumstances, damage in the form of cracks still accumulates, but at the microscopic level.

The ultimate stress, max$|\sigma_1 - \sigma_3|$, is plotted against σ_3 in Figure 2. This rock shows little scatter about the best fit straight line, and the strength is well represented by max$|\sigma_1 - \sigma_3| = 177 + 2.11\sigma_3$. All strength data are given in Table 2.

The two hydrostats for the sandstone obtained before the 200 MPa-confining pressure triaxial tests are displayed in Figure 3. These curves are typical of rocks like sandstone that have some initial porosity. Thus, the sandstone shows an increasing bulk modulus with increasing pressure as cracks close.

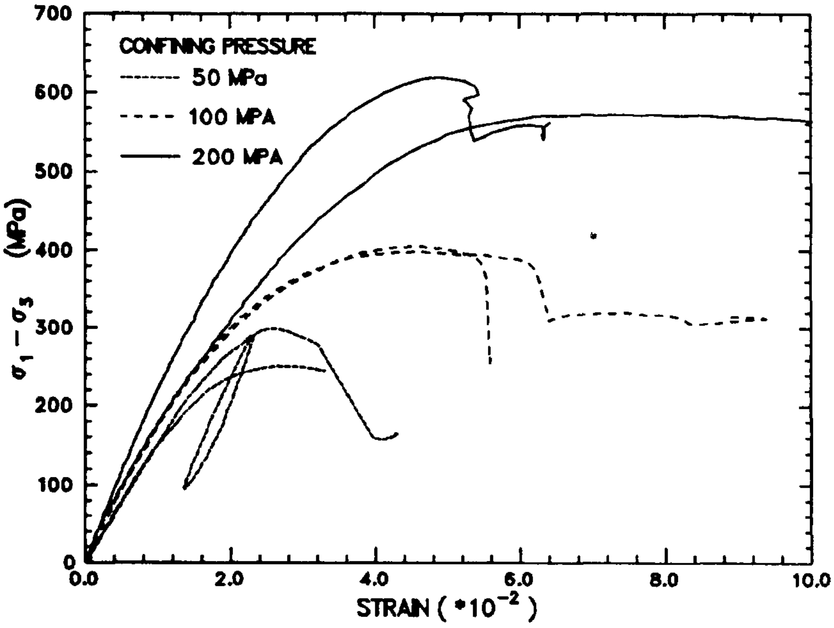

Figure 1: Stress-strain curves for sandstone.

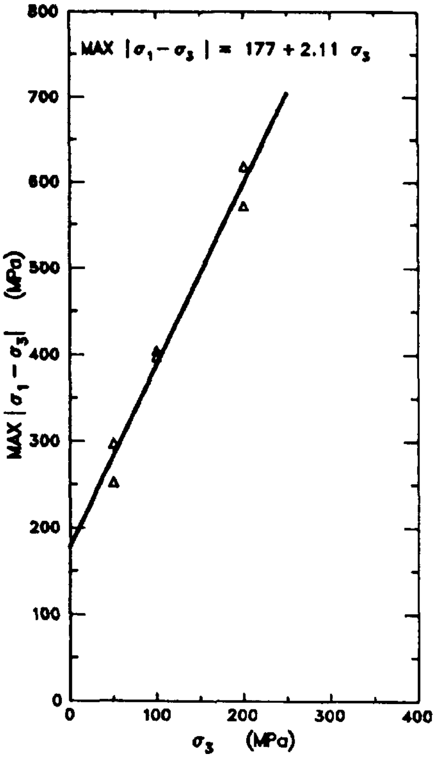

Figure 2: Failure criterion for sandstone.

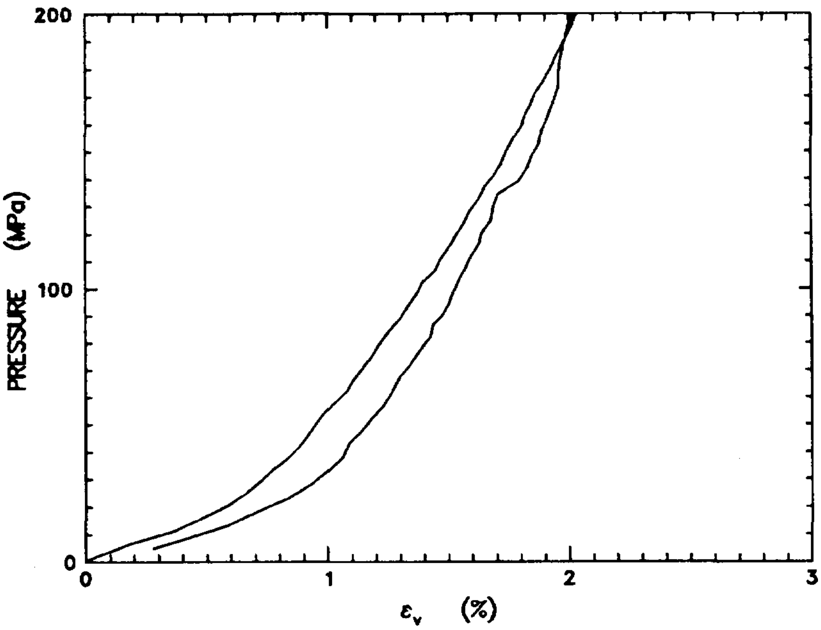

Figure 3: Hydrostats for sandstone.

3.2 Granite

The mechanical properties of the granite were much affected by its large variations in grain size, foliations, and healed fractures. The failure criterion is shown in Figure 4; note the large scatter. The tabulated data are from the first block delivered, which had a visible layering. The blocks delivered later did not have such layering; these were not tested. As can be seen from Tables 3 and 4, the layering has a notable effect on the strength. Although not tested, the strength of the unfoliated material is probably closer to that of the 90-degree tests. The Young's modulus is likely to be somewhat higher than that shown for the 90-degree tests. In addition to the foliation, we found many fine fractures cemented with some undetermined mineral. These fractures probably contribute to scatter in the test results. They certainly have strong effect on the tensile properties, which will be reported subsequently.

Poisson ratio data for the 30-degree samples does not appear meaningful and therefore was not listed. Also, the Young's modulus for these samples is only an apparent one because of the anisotropy.

The dynamic compressive strength is given in Table 5 for four samples of granite tested in the Kolsky bar. The strength was 175 to 330% greater than the quasi-static value, depending on rate. In addition, I measured the p-wave velocity to be 5.050 and 4.618 mm/μs for two samples of the nonfoliated granite.

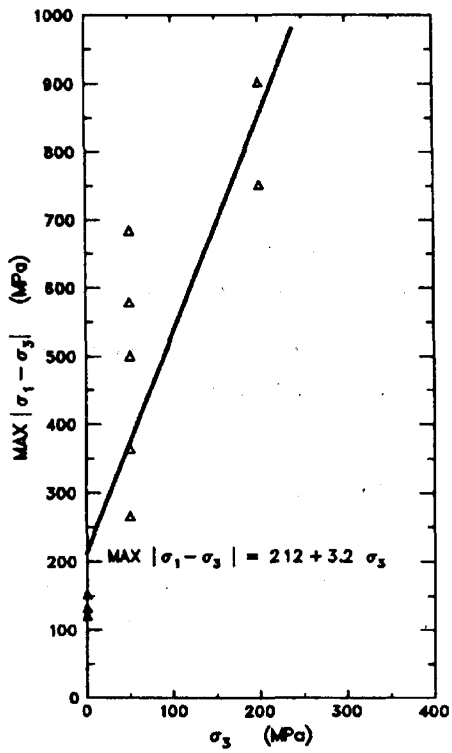

Figure 4: Failure criterion for granite.

4 Conclusions

Some basic quasi-static and dynamic mechanical properties of a sandstone and a granite have been measured. Both rocks have linear failure criteria, and exhibit faulting in the post-peak region of the stress-strain curve. The sandstone is more consistent in its properties than the granite because it is petrofabrically more uniform. The strength of the granite when loaded at 30 deg to the layering was only 65% of the strength measured normal to the layering. The sandstone, which possessed sedimentary layering, showed a 20% difference in p-wave velocity between measurements normal to and parallel to the bedding. Its strength variation with orientation was not measured. Strain-rate effects were measured in compression on the granite, and it was found that the impulsively loaded samples could be as much as 330% stronger than those quasi-statically loaded.

5 Acknowledgement

Tom Tormey assisted with all aspects of the experiments.

6 References

1. Holcomb, D. J. and A. K. Jones, Data Acquisition for the Rock Mechanics Lab, *SAND83-0646*, Sandia National Laboratories, Albuquerque, NM, 1983.

2. Holcomb, D. J. and M. J. McNamee, Displacement Gage for the Rock Mechanics Laboratory, *SAND84-0651*, Sandia National Laboratories, Albuquerque, NM, 1984.

3. Kolsky, H., An investigation of the mechanical properties of materials at very high rates of loading, *Proc. Phys. Soc.* **B62**, 676–700 (1949).

4. Selleck, C. B., Graph II: A Digitizing and Graph Plotting Program, *SAND84-0302*, Sandia National Laboratories, Albuquerque, NM, 1984.

A Tabulated data.

Table 1: Densities and compressional wave speeds for sandstone.

Sample ID	Hole	Depth (m)	ρ (g/cm^3)	$v_\perp$ (mm/μs)	$v_\parallel$ (mm/μs)	$\frac{(v_\parallel - v_\perp)}{v_{mean}}$ (%)
B	EXPL-2	4.267-4.445	2.523	2.77	3.18	13.8
C	EXPL-1	5.588-5.690	2.590	2.81	3.33	16.9
D	"	5.690-5.817	2.593	2.84	3.57	22.8
E	"	5.817-5.944	2.601	2.80	3.17	12.4
F	"	5.944-6.096	2.599	2.86	3.30	16.0
G	"	4.978-5.105	2.621	2.83	3.70	26.6
H	"	5.105-5.207	2.603	2.77	3.22	15.0
I	"	5.207-5.334	2.576	2.72	3.63	28.7
J	"	5.334-5.486	2.596	2.76	3.45	22.2
Ave.±s.d.			2.589±0.028	2.80±0.04	3.39±0.20	19.38±5.81

Table 2: Triaxial data for sandstone.

Sample ID	σ_3 (MPa)	$\sigma_1 - \sigma_3$ (MPa)	ν	E (GPa)
B	50	296	0.12	15.2
D	50	251	0.10	14.8
C	100	403	-	-
G	100	396	0.12	15.8
F	200	617	0.12	21.0
H	200	570	0.10	14.8

Table 3: Uniaxial compression data for granite.

Sample Number	θ (deg)	ρ (g/cm^3)	Maximum σ_1 (MPa)	E (GPa)	ν
1901	90	2.68	131	55.5	0.28
1902	90	2.67	119	48.8	0.34
1903	90	2.67	150	55.4	0.25
Ave.±s.d.			133 ± 16	53.2 ± 3.8	0.29 ± 0.05
1601	30	2.67	93.5	54.5	
1602	30	2.65	71.2	18.8	
1603	30	2.66	86.5	45.4	
1604	30	2.65	89.4	37.9	
1605	30	2.66	87.9	36.9	
Ave.±s.d.			85.7 ± 8.5	38.7 ± 13.2	

Table 4: Triaxial compression at 50 MPa confining pressure for granite.

Sample Number	θ (deg)	ρ (g/cm^3)	Maximum $(\sigma_1 - \sigma_3)$ (MPa)	E (Gpa)
G1905	90	2.68	362	62.5
G2902	90	2.68	264	77.7
G2903	90	2.71	577	71.2
G2905	90	2.70	682	83.8
G2906	90	2.70	499	90.6
Ave.±s.d.			476.8±166.7	77.2 ± 10.9
G1607	30	2.73	337	57.8
G1608	30	2.67	350	75.3
G6301	30	2.70	481	74.0
G6302	30	2.69	457	68.8
Ave.±s.d.			406±73	69.0 ± 8.0

Table 5: Dynamic compressive strength of granite.

Sample Number	Maximum σ_1 (MPa)	Strain Rate (s^{-1})
G1901K	230.0	113
G1902K	314.7	135
G1904K	335.6	167
G2902K	449.0	192

Distribution:

Mike Barber
Atlas Powder Company
P.O. Box 271
Tamaqua, PA 18252

R. Frank Chiappetta
Blasting Analysis International
1932 South Fourth Street, Suite M-31
Allentown, PA 18103

R. Cena
Lawrence Livermore National Laboratory
P.O. 808
Livermore, CA 94550

Laramie Project Office (2)
U.S. Dept. of Energy
P.O. Box 1189
Laramie, WY 82070
    C. Roosmagi
    T. C. Bartke

Morgantown Energy Technology Center (2)
U.S. Dept. of Energy
P.O. Box 880
3610 Collins Ferry Road
Morgantown, WV 26507-0880
    H. Guthrie
    J. Burchfield

Oil, Gas & Shale Technology (2)
U.S. Dept. of Energy
Mail Stop FE-33, GTN
Washington, DC 20545
    J. W. Ramsey
    H. E. Thomas

Richard Smith
EG & G Idaho Inc.
Box 625, MS2212
Idaho Falls, ID 83415

U.S. Bureau of Mines (3)
Twin Cities Research Center
5629 Minnehaha Avenue South
Minneapolis, MN 55117
    M. Stagg
    S. Crum
    S. Rohl

J. Virgona
U.S. Dept. of Energy
P.O. Box 2567
Grand Junction, CO 81502

Sandia Internal:

1510 J. W. Nunziato
1511 D. K. Gartling
1520 L. W. Davison
1521 R. D. Krieg
1522 R. C. Reuter
1523 J. H. Biffle
1523 J. Jung
1524 L. W. Davison, acting
1530 D. B. Hayes
3141 S. A. Landenberger (5)
3151 W. I. Klein (3)
3154-1 C. L. Ward, For: DOE/TIC (8)
6000 D. L. Hartley
6200 V. L. Dugan
6210 B. W. Marshall
6230 W. C. Luth
6232 W. R. Wawersik
6232 W. A. Olsson (5)
6250 R. K. Traeger
6258 P. J. Hommert (5)
6258 D. S. Preece
6258 B. J. Thorne
8524 J. A. Wackerly